Journal of Molecular Structure 984 (2010) 137–145

Contents lists available at ScienceDirect

Journal of Molecular Structure

journal homepage: www.elsevier.com/locate/molstruc

Experimental and theoretical studies of the molecular structure of 4-(3-(1*H*-imidazol-1-yl)propyl)-5-*p*-tolyl-2*H*-1,2,4-triazol-3(4*H*)-one

Reşat Ustabaş [a], Nevin Süleymanoğlu [b,*], Hasan Tanak [c], Yelda Bingöl Alpaslan [c], Yasemin Ünver [d], Kemal Sancak [d]

[a] Department of Middle Education, Educational Faculty, Ondokuz Mayıs University, 55200 Atakum, Samsun, Turkey
[b] Atatürk Vocational High School, Gazi University, 06760 Çubuk, Ankara, Turkey
[c] Department of Physics, Faculty of Arts & Science, Ondokuz Mayıs University, 55139 Kurupelit, Samsun, Turkey
[d] Department of Chemistry, Faculty of Arts and Sciences, Karadeniz Teknik University, 61080-Trabzon, Turkey

ARTICLE INFO

Article history:
Received 10 June 2010
Received in revised form 5 August 2010
Accepted 15 September 2010
Available online 29 September 2010

Keywords:
1,2,4-Triazol
Imidazol
IR and NMR spectroscopy
Density functional theory
Molecular electrostatic potential

ABSTRACT

The triazol–imidazol compound, 4-(3-(1*H*-imidazol-1-yl)propyl)-5-*p*-tolyl-2*H*-1,2,4-triazol-3(4*H*)-one (**3**), ($C_{15}H_{17}N_5O$), was prepared and characterized by ^{1}H NMR, ^{13}C NMR, IR and single-crystal X-ray diffraction. By using the density functional theory (DFT) method with 6-31G(d) basis set, the molecular geometry, vibrational frequencies and gauge including atomic orbital (GIAO) ^{1}H and ^{13}C NMR chemical shift values of the title compound (**3**) in the ground state were calculated and compared with the experimental data. The calculated results are show that the optimized geometry can well reproduce the crystal structure. X-ray, FT-IR and NMR spectral results of the title compound (**3**) indicate that the compound exists as keto form. To determine most favorable conformation as theoretically, molecular energy profile of the title compound (**3**) were obtained as a function of the selected torsion angles T(N1—C8—C7—C6), T1 and T(C8—N1—C10—C11), T2, which is varied from −180° to +180° in every 10 by semi-empirical (PM3) calculations. In addition, DFT calculations of the title compound (**3**), molecular electrostatic potential and frontier molecular orbitals were performed at B3LYP/6-31G(d) level of theory.

1. Introduction

1,2,4-Triazole derivatives have been reported as fungicidal [1], insecticidal [2], antimicrobial compounds [3] and some showed antitumor activity [4,5] or are anticonvulsants [6], antidepressants [7] and plant growth regulator anticoagulants [8]. It was reported that compounds having triazole moieties such as vorozole, anastrozole and letrozole appear to be very effective aromatase inhibitors, which are very useful for preventing breast cancer [9–11]. The considerable biological importance of imidazoles and triazoles has stimulated much work on these heterocycles and there are a variety of methods available for the synthesis of 1,2,4-triazole [12]. 1,2,4-Triazole and imidazole are the hetero-rings of choice and are essential structural features of many of the potent azole fungicides [13]. It is also known that the triazole ring has been used instead of imidazole, which is found in the structure of some antagonist, anti-ulcer and antifungal drugs [14]. Ionic liquids, of which imidazolium salts are most widely used, have gained initial notice of synthetic chemists as environmentally friendly organic solvents, and continue to hold their attention as reaction catalysts or promoters. Additionally, They have the ability to dissolve an enormous range of inorganic, organic, and polymeric materials at very high concentrations, are noncorrosive, and have low viscosities and no significant vapor pressures [15].

The main goal of our study is to synthesize the triazole compound containing imidazol which are fundamental compounds in the preparation of ionic liquids and used as a antimicrobial substance. There are both keto form and hydroxyl form of 1,2,4-triazol in the theoretical but, keto form is more dominant form. In addition, IR and NMR spectral datas show that, while keto form is available, hydroxyl form is not existed [16]. In this study, we present results of a detailed investigation of the synthesis and structural characterization of 4-(3-(1*H*-imidazol-1-yl)propyl)-5-*p*-tolyl-2*H*-1,2,4-triazol-3(4*H*)-one (**3**), ($C_{15}H_{17}N_5O$), using single-crystal X-ray diffraction, IR-NMR spectroscopy and quantum chemical methods. The geometrical parameters, fundamental frequencies and GIAO ^{1}H and ^{13}C NMR chemical shift values of the title compound (**3**) in the ground state have been calculated by using the DFT (B3LYP) method with 6-31G(d) basis set, and compared with experimental data. The spectral datas of the title compound (**3**) show that the compound exists as keto form.

* Corresponding author.
E-mail address: nsuleymanoglu@gazi.edu.tr (N. Süleymanoğlu).

0022-2860/$ - see front matter © 2010 Elsevier B.V. All rights reserved.
doi:10.1016/j.molstruc.2010.09.018

2. Experimental and computational methods

2.1. Experimental

2.1.1. Physical measurements

In the determination of the melting point, a Gallenkamp melting point apparatus was used. By means of a Perkin-Elmer 1600 series FT-IR spectrophotometer using KBr pellets, the IR spectrum of the title compound were recorded in the range 4000–400 cm^{-1} region. And finally, The ^1H-, and ^{13}C-Nuclear Magnetic Resonance spectra were recorded on a Varian-Mercury 200 MHz spectrometer, where TMS as an internal standard and DMSO-d6 as solvent are used. For elemental analysis, combustion/gas chromatography method was used. Elemental analyses were performed on a Hewlett–Packard 185 CHN analyzer; their values agreed with the calculated ones. A selected crystal with colourless and dimensions of 0.60 × 0.59 × 0.46 mm was mounted on a STOE IPDS II X-ray diffractometer. Data collection was performed at room temperature (293 K) using graphite monochromated Mo Kα radiation (λ = 0.71073 Å). The cell parameters were determined by using X-AREA software [17]. The crystal structure was solved by direct methods using SHELXS-97 [18]. Molecular plot was prepared with *ORTEPIII* for Windows [19]. *WinGX* software [20] was used to prepare material for publication. Details of the data collection conditions and the parameters of refinement process are given in Table 1.

Table 1
Crystal data and structure refinement parameters for the title compound **(3)**.

Crystal data	
Chemical formula	$C_{15}H_{17}N_5O$
M_r	283.34
Cell setting, space group	Orthorhombic, *Pbca*
Temperature (K)	293
a, *b*, *c* (Å)	8.4234 (19), 32.3591 (3), 10.6577 (7)
V (Å^3)	2905.0 (7)
Z	8
D_x(Mg cm^{-3})	1.296
Radiation type	Mo Kα
μ (mm^{-1})	0.09
Crystal form, colour	Prism, colourless
Crystal size (mm^3)	0.60 × 0.59 × 0.46
Data collection	
Diffractometer	STOE IPDS 2
Data collection method	Scans method
No. of measured, independent and observed reflections	43,108, 2750, 2312
Criterion for observed reflections	$I > 2\sigma(I)$
R_{int}	0.057
θ_{max}	25.7°
Refinement	
Refinement on	F^2
$R[F^2 > 2\sigma(F^2)]$, $wR(F^2)$, S	0.039, 0.112, 1.08
No. of reflection	2750 reflections
No. of parameters	192
H-atom treatment	Constrained to parent site
Weighting scheme	$w = 1/[\sigma^2(F_0^2)+(0.0652P)^2 + 0.2022P]$ $P=(F_0^2 + 2F_c^2)/3$
$(\Delta/\sigma)_{max}$	0.001
$\Delta\rho_{max}$, $\Delta\rho_{min}$ (e Å^{-3})	0.13, −0.14

2.1.2. Synthesis

Ethyl 2-(-ethoxy(p-tolyl)methylene] hydrazine carboxylate (**1**) (2.50 g, 10 mmol) together with N-(3-aminopropyl) imidazole (**2**) (1.25 g, 10 mmol) were heated without solvent in a sealed tube for 2 h at 160–180°. Then, the mixture was cooled to r.t. and a solid formed. The crude product was recrystallized using acetone/petroleum ether (1:2) (yield 70.20%) to afford the title compound (**3**). M.P, 456–457 K. Anal. calc. for $C_{15}H_{17}N_5O$: C, 63.59; H, 6.05; N, 24.72. Found: C, 63.65; H, 6.11; N, 24.79. EI-MS: 283.33 $[M]^+$. Synthetic pathway of the title compound (**3**) is shown in Scheme 1.

2.2. Computational methods

DFT and PM3 calculations were carried out using *GAUSSIAN03* [21] program package. The geometry optimizations were performed by using DFT *ab initio* method, starting from the experimental structures. DFT calculations are performed without any constraints on the molecule using the B3LYP hybrid exchange–correlation function [22] with the aid of the 6-31G(d) basic set. The conformational preferring of the title compound (**3**) is determined by conformational analysis, selected degree of torsional freedoms, T1 and T2 were varied from −180° to +180° in steps of 10°, and molecular energy profiles were obtained at the semi-empirical PM3 level [23,24]. B3LYP/6-31G(d) were used for the calculations of the MEP [25–28] and frontier molecular orbitals (FMOs) were carried out with the same level of theory B3LYP/6-31G(d). The calculation of harmonic frequencies for the optimized geometry were made at the same level and these were scaled by 0.9613 [29]. After that, by using Gauss-View molecular visualization program [30], the vibrational bands were assigned. Both the geometry of title compound (**3**) and the geometry of tetramethylsilane (TMS) are optimized. ^1H and ^{13}C NMR chemical shifts are calculated. For this calculation, the standard GIAO/B3LYP/6-31G(d) (Gauge-Independent Atomic Orbital) approach [31,32] with the program package Gaussian 03W are used. In order to convert the ^1H- and ^{13}C-NMR chemical shifts to TMS scale, the calculated absolute chemical shielding of TMS are subtracted from these values. The calculated absolute chemical shielding of TMS are 32.2 ppm and 189.84 ppm for B3LYP/6-31G(d), respectively.

3. Results and discussion

The synthesis of 4-(3-(1*H*-imidazol-1-yl)propyl)-5-*p*-tolyl-2*H*-1,2,4-triazol-3(4*H*)-one (**3**) was obtained by the reaction of compounds **1** and compound **2** (Scheme 1).The reaction pathway is show that reaction started amino group of compound **2** attacked carbonyl group of compound **1** with nucleophilic substitution

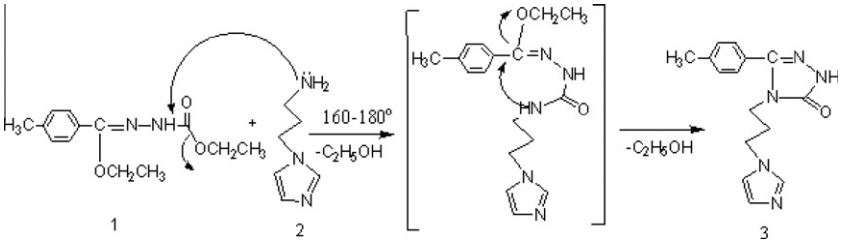

Scheme 1. Synthetic pathway for the preparation of the title compound **(3)**.

reaction. Then, same amino group attack to imino carbon atom to obtain triazol ring. Spectroscopic data of the product **3** confirmed the success of the cyclization reaction. The EI–MS of compound **3** confirmed the proposed structure with a molecular ion peak at $m/z = 283.33$. 1,2,4-Triazoles with exocyclic double bond can be considered to exist in a tautomeric equilibrium between keto (O═C—NH) and hydroxy (HO—C═N) forms [33]. The IR datas indicated the formation of compound **3** by the disappearance of C—O stretching vibrations at 1235 cm^{-1}, and C═O belonging to the triazole at 1710 cm^{-1}. The signal observed at 3383 cm^{-1} in the IR spectra of compound **3** was attributed to the N—H of triazol. In the ^1H NMR spectra, the existence of **3** was revealed by the disappearance of form of the ester CH_2O groups (4.36–4.40 ppm) in the precursor (**1**) after the cyclization and the appearance of a new peak at 11.80 ppm integrating for one H-atom (exchangeable with D_2O) belonging to H—N [15]. More detailed information about the structure of compound **3** was provided by the ^{13}C NMR spectra. The signals for the triazole C(8) and the C═O group C(9) are found at 146.49 and 155.63 ppm, respectively. FT-IR, ^1H and ^{13}C NMR spectral datas of the title compound **(3)** show us that the compound exists as keto form.

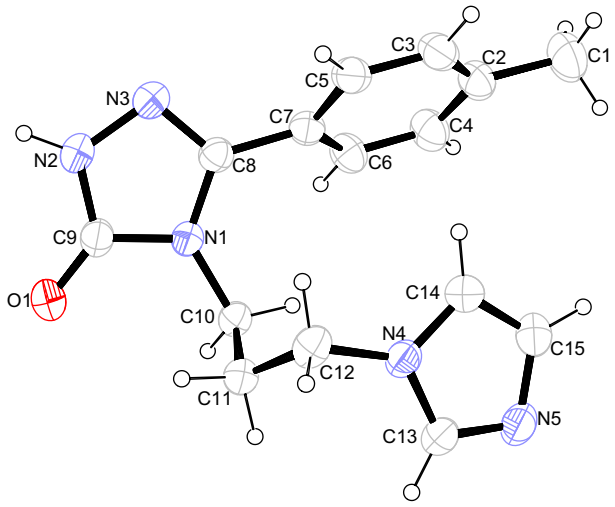

Fig. 1. An *ORTEP* drawing of the title compound **(3)**, with the atom numbering scheme. Displacement ellipsoids are drawn at the 30% probability level.

Table 2
Hydrogen-bond geometry (Å, °).

D—H···A	D—H	H···A	D···A	D—H···A
C13—H13···O1^{i}	0.93	2.53	3.401 (2)	157
C12—H12B···O1^{ii}	0.97	2.54	3.437 (2)	154
N2—H2···N5^{iii}	0.86	1.99	2.816 (2)	162

Note: D: donor, A: acceptor. Symmetry transformations used to generate equivalent atoms. (i) $-x, -y+1, -z$; (ii) $-x+1/2, -y+1, z-1/2$; (iii) $x, y, z+1$.

3.1. Description of the crystal structure

The title compound (**3**) crystallizes in the orthorhombic, *Pbca* space group *with* $Z = 8$ in the unit cell. Fig. 1 shows ORTEPIII diagram of the title compound (**3**) with the atom numbering scheme. As revealed by X-ray structure analysis, each of tree rings in the title compound (**3**) remains planar itself. The dihedral angles between triazol and benzene, triazol and imidazol rings are 53.58 (6)° and 15.62 (6)°, respectively. Methyl atom C1 deviates from the benzene ring plane by 0.0309 (2) Å. The deviations from triazol ring plane of atom O1 is −0.0361 (11) Å. The observed bond distances from X-ray analysis agree well with similar bonds reported in the literature [34–36].

The crystal structure is stabilized by intermolecular interactions and π–π stacking interaction. In crystal structure of the title compound (**3**), there are three intermolecular hydrogen bonds (Table 2). The donor and acceptor distances are 2.816(2) (2) Å for N2—H2—N5 [symmetry code: $x, y, z+1$], 3.437 (2) Å for C12—H12—O1 [symmetry code: $-x+1/2, -y+1, z-1/2$] and 3.401(2) Å for C13—H13—O1 [symmetry code: $-x, -y+1, -z$;]; respectively. Figs. 2a, 2b and 2c show forming of the sheet structures along the different directions. On the other hand, there is two intermolecular π–π stacking interaction occurring between the triazole rings and imidazole rings [(*Cg*1···*Cg*1 = 4.213 (13) Å; symmetry code: $-1/2+x, y, 1/2-z$); (*Cg*2···*Cg*2 = 4.265 (14) Å; symmetry code: $-1/2+x, y, 3/2-z$)]. Intermolecular hydrogen-bonding and π–π stacking interactions in the crystal structure are the most important feature in terms of supramolecular environment of the title compound (**3**).

3.2. Optimized geometry and conformational analysis

The first step for computational studies of the title compound (**3**) was to determine the optimized geometry. The molecular geometry without any restrictions from the results of X-ray diffrac-

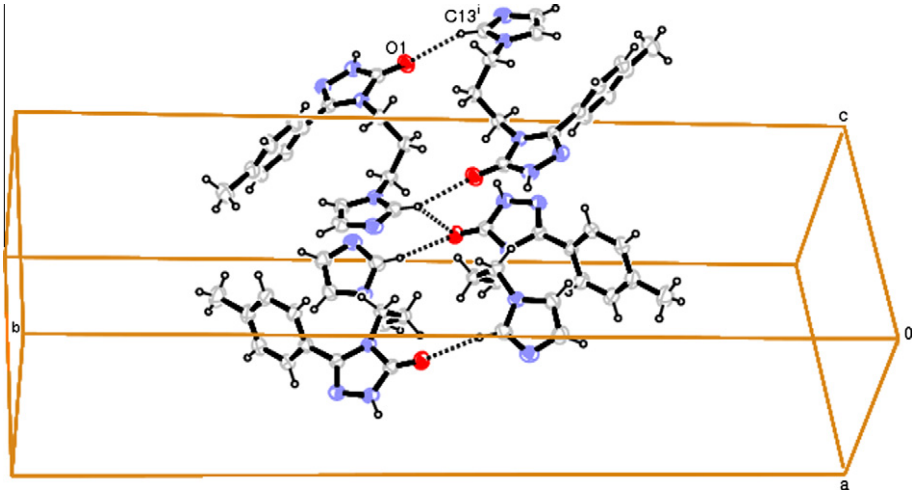

Fig. 2a. The compound (**3**) linked by C13-H13···O1^{i} (i: $-x, -y+1, -z$) hydrogen bond along the ab plane.

tion experimental were obtained. The second step, B3LYP (Becke's three parameter hybrid functional using the LYP correlation functional) calculations at basis set 6-31G(d) [37].

The selected bond lengths, bond angles and torsion angles are listed in Table 3 and compared with the experimental data of the title compound (**3**). When the X-ray structure of the title compound (**3**) is contrasted with its DFT optimized counterpart (Fig. 3), it can be easily seen that they are slightly different each other. Because, experimental results are based on the molecules in the solid state while theoretical calculations are based on the isolated molecules in the gas-phase. The RMSE fit of the atomic position of the title compound (**3**) to those of its DFT optimized counterpart is 0.0543 Å. As compared to experimental and calculated results, the biggest deviation of the bond lengths is

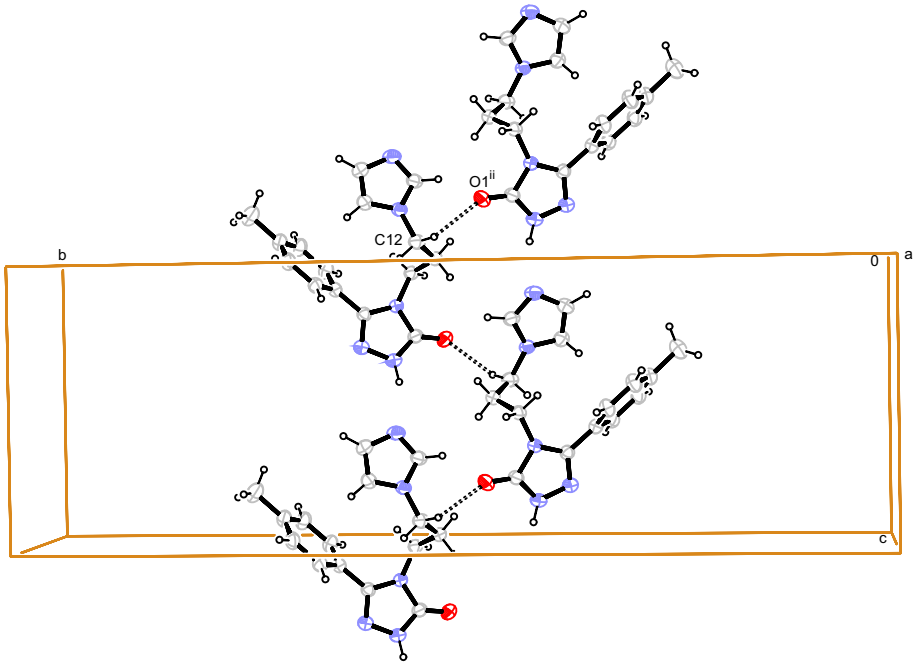

Fig. 2b. The compound (**3**) linked by C12-H12B···O1^{ii} (ii: $-x + 1/2, -y + 1, z - 1/2$) hydrogen bond along the c axes.

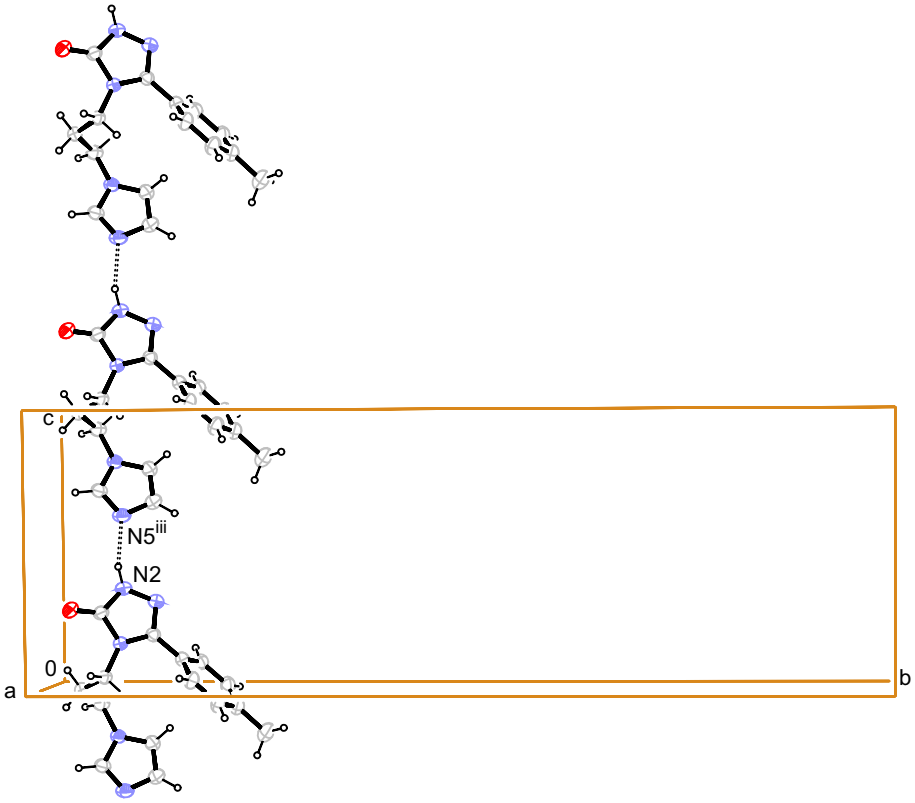

Fig. 2c. The compound (**3**) linked by N2-H2···N5^{iii} (iii: $x, y, z + 1$) hydrogen bond along the *c* axes.

Table 3
Selected molecular structure parameters.

Parameters	Experimental	B3LYP 6-31G(d)
Bond lengths (Å)		
N1—C8	1.3744 (16)	1.3927
N1—C9	1.3896 (16)	1.4035
N1—C10	1.4571 (16)	1.4676
N2—C9	1.3453 (18)	1.3735
N2—N3	1.3850 (16)	1.3739
O1—C9	1.2274 (17)	1.2271
N4—C13	1.3410(18)	1.3700
N3—C8	1.3052 (17)	1.3085
N5—C15	1.366 (2)	1.3767
C15—C14	1.344 (2)	1.3757
C12—C11	1.510 (2)	1.536
Bond angles (°)		
C8—N1—C9	107.64 (11)	107.79
C8—N1—C10	130.88 (11)	130.68
C9—N1—C10	121.36 (11)	121.46
N3—C8—N1	111.64 (12)	111.33
N4—C12—C11	111.50 (12)	113.97
Torsion angles (°)		
C10—N1—C8—C7	9.5 (2)	6.14
C8—N1—C10—C11	99.86 (16)	116.96
N1—C8—C7—C6	51.55 (19)	45.62
C10—N1—C8—N3	−175.06(13)	−175.18
N3—N2—C9—O1	−178.31 (15)	−177.70

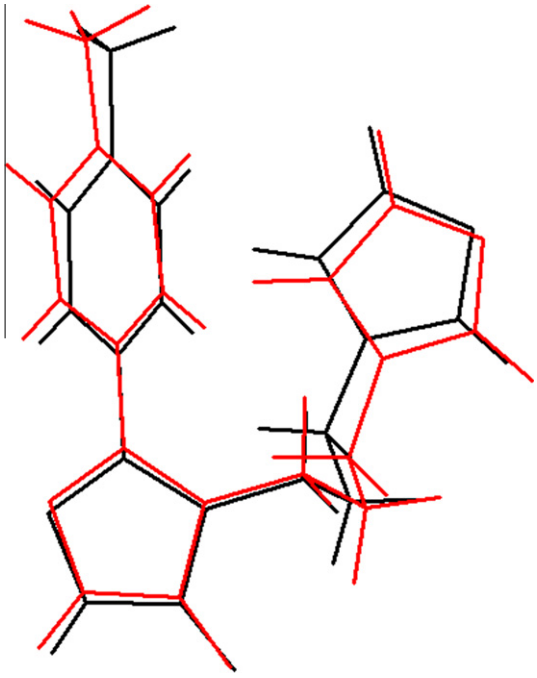

Fig. 3. Atom-by-atom superimposition of the structures calculated (red) over the X-ray structure (black) for the title compound **(3)**. (For interpretation of the references to colour in this figure legend, the reader is referred to the web version of this article.)

0.032 Å at C15—C14 and the biggest deviation of the bond angles is 2.47° at N4—C12—C11. In the optimized geometry, the dihedral angles between triazol and benzene, triazol and imidazol rings are 44.35° and 19.55°, respectively. The torsion angles C10—N1—C8—C7, C8—N1—C10—C11 and N1—C8—C7—C6 obtained from DFT are 6.14°, 116.96° and 45.62°, respectively.

In order to define the preferential position of imidazol and benzene rings, conformational analysis was carried out using PM3 computations as a function of the selected degrees of torsional freedom T(N1—C8—C7—C6), T1 and T(C8—N1—C10—C11), T2 varied from −180° to and 180° in step of 10°. The calculated energy profiles versus the selected torsion angles T1 and T2 are shown in Fig. 4. The respective values of the selected degrees of torsional freedom, T1 and T2 are 51.55(19)° and 99.86(16)° in X-ray structure, whereas the corresponding values in DFT optimized geometry are 45.62° and 116.96°, respectively. These calculated values are in good agreement with the experimental values.

As can be seen in Fig. 4, the low energy domains for T1 are located at −130° and 50° having energy of 45.20 and 45.00 kcal/mol, while they are located at −90° and 80° having energy of 45.48 and 44.96 kcal/mol, respectively, for T2. Energy difference between the most favorable and unfavorable conformers, which arises from rotational potential barrier calculated with respect to the two selected torsion angles, is calculated as 89.79 kcal/mol for T1 and as 51.47 kcal/mol for T2, when both selected degrees of torsional freedom are considered.

As compared to the rotation around the torsion angle along the C8—C7 bond (T1) and the torsion angle along the N1—C10 bond (T2), it can be said that this high potential barrier observed for T1 is due to steric hindrances between benzene ring and the imidazol ring. Even so, it can be stated that the contribution to molecular energy of torsion angle T1 is more than T2.

3.3. Vibrational spectra

Harmonic vibrational frequencies calculated by using DFT/B3LYP with 6-31G(d) basic set are given in Table 4, together with

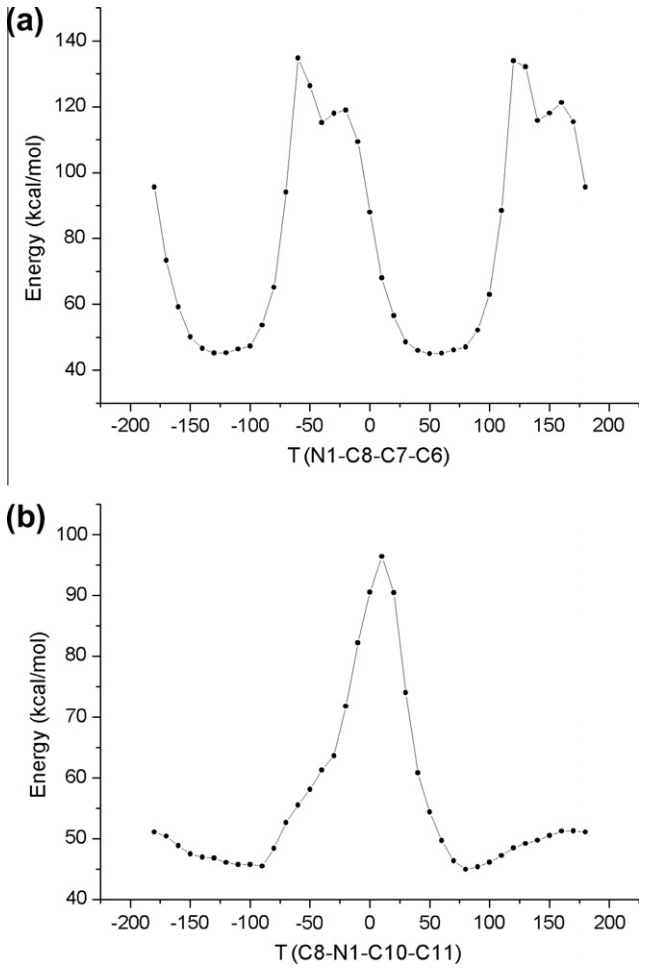

Fig. 4. Molecular energy profiles of the optimized counterpart of the title compound **(3)** against the selected degrees of torsional freedom T(N1—C8—C7—C6), T1, and T(C8—N1—C10—C11), T2, respectively.

Table 4
Comparison of the experimental and calculated vibrational frequencies (cm^{-1}).

Assignments[a]	Experiment	B3LYP/6-31G(d)
ν(N—H)	3383	3539
ν_{ring}(C—H)	3155–3116	3166–3133
ν_{as}(C—H_3)	3001	3009
ν_s(C—H_2)	2971	2955
ν(C = O)	1710	1759
ν(C = C) + ν(C = N) + γ_{ring}(C—H)	1515	1501
α(C—H_2) + γ_{ring}(C—H)	1453	1452
ω(CH_2—CH_2) + ν(C—N) + γ(N—H)	1351	1348
ν(C—N) + δ(C—H_2)	1233	1217
γ_{ring}(C—H) + δ(C—H_2) + ν(C—N)	1105	1105
ω(C—H_3) + γ_{ring}(C—H)	977	981
ω_{ring}(C—H) + ω(C—H_3)	823	811
ω_{ring}(C—H)	776	772
ω_{ring}(C—H) + ω(C—H_3)	737	710

[a] ν, stretching; β, bending; α, scissoring; γ, rocking; ω, wagging; δ, twisting; s, symmetric; as, asymmetric.

their experimental results. The FT-IR spectrum of the title compound (**3**) is shown in Fig. 5. As can be seen in Table 4, The N—H stretching mode, calculated as 3539 cm^{-1}, was observed at 3383 cm^{-1} in the FT-IR spectrum. This difference between experimental and calculated N—H stretching vibrations (156 cm^{-1}) can be due to N2—H2···N5 strong intermolecular hydrogen bond, that calculations do not take into consideration. In the literature, the some N—H stretching modes observed for the different substituent-triazole ring are 3470 cm^{-1} [38] and 3417 cm^{-1} [39] as experimentally, and 3501 cm^{-1} for B3LYP/6-311G(d,p) level [39] and 3566 cm^{-1} [40] for B3LYP/6-31G(d). The C—H aromatic stretching modes were calculated as 3166–3133 cm^{-1}, that were observed at 3155–3116 cm^{-1} (Table 4). The stretching C=O vibration gives rise a band at 1710 cm^{-1} in the infrared experimental spectrum, while the calculated value is predicted 49 cm^{-1} higher, at 1759 cm^{-1}. This difference given for C=O stretching vibration can be explained by the existence of the C—H···O intermolecular hydrogen bonds given in Table 2, because isolated molecules are taken into consideration in calculations. The two bands attributed to the C=N stretching vibrations, obtained at 1575 and 1515 cm^{-1}, were calculated as 1566 and 1501 cm^{-1}, respectively (Table 4). The above conclusions are in good agreement with the similar triazole compounds [40,41].

Experimental frequencies of the title compound (**3**) were compared with calculated vibrational frequencies by correlation

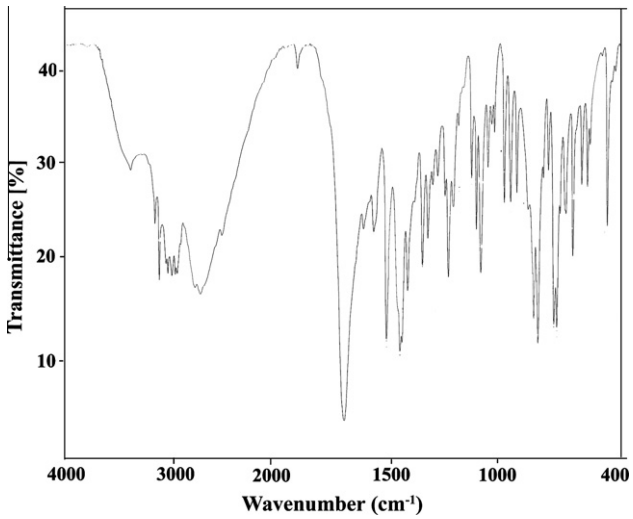

Fig. 5. FT-IR spectrum of the title compound (**3**).

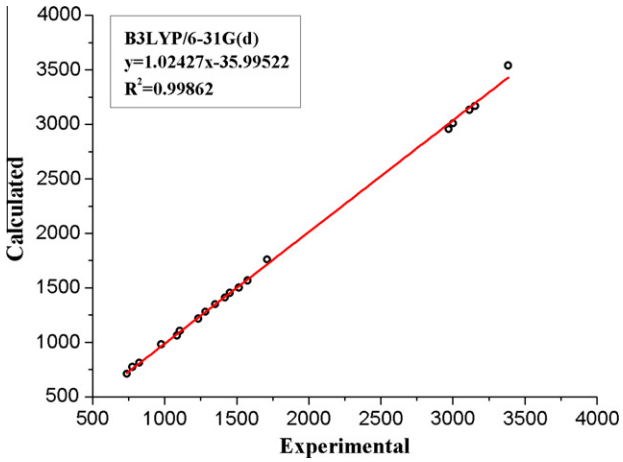

Fig. 6. Correlation graphic of calculated and experimental frequencies of the title compound (**3**).

graphics given in Fig. 6. The correlation graphics in Fig. 6 shows that experimental fundamentals are found to have a good correlation with calculations. Our estimations on N—H stretching mode contain ~4.0% error on an average for B3LYP level. The other modes in our results are estimated in a smaller error range.

3.4. NMR spectra

GIAO ^1H and ^{13}C chemical shift values (with respect to TMS) calculated by the B3LYP method with 6-31G(d) basis set were compared to the experimental ^1H and ^{13}C chemical shift values. The results are given in Table 5.

Table 5
Theoretical and experimental ^1H and ^{13}C isotropic chemical shifts (with respect to TMS, all values in ppm) for the title compound **(3)**.

Atom	Experimental (ppm) (DMSO-d_6)	Calculated (ppm) B3LYP/6-31G(d)
C1	21.11	22.14
C2	124.73	134.34
C3	127.81	124.24
C4	127.81	123.07
C5	129.71	123.54
C6	129.71	121.74
C7	140.31	119.92
C8	146.49	141.74
C9	155.63	143.25
C10	60.53	40.34
C11	30.20	30.59
C12	43.65	42.45
C13	140.11	127.05
C14	119.62	113.14
C15	129.92	121.67
H1A	2.36	1.95
H1B	2.36	2.56
H1C	2.36	2.62
H2	11.80	6.80
H3	7.29	7.26
H4	7.29	7.25
H5	7.44	7.63
H6	7.44	7.04
H10A	3.93	3.66
H10B	3.93	3.65
H11A	2.15–2.20	1.43
H11B	2.15–2.20	3.01
H12A	3.63	3.23
H12B	3.63	3.70
H13	7.57	6.9
H14	7.12	5.03
H15	6.87	6.29

^{1}H chemical shift values (with respect to TMS) have calculated to be 7.63–1.43 ppm at B3LYP/6-31G(d) level, whereas the experimental results are observed to be 11.80–2.15 ppm shown in Fig. 7. The C(1)H_3 protons of the title compound gave a singlet at 2.36 ppm. This statement was calculated at 1.95–2.62 ppm at B3LYP level. The C—H signals of imidazole ring were observed at 7.57, 7.12 and 6.87 ppm. The N—H hydrogen in the 1,2,4-triazole ring appears at 11.80 ppm, while this signal is observed computationally at 6.80 ppm (Table 5). This considerable difference between experimental and calculated chemical shifts is due to N2—H2···N5 strong intermolecular hydrogen bond, such as in the IR spectrum, since the theoretical calculations are based on isolated molecules in the gas-phase. In different substituent-1,2,4-triazole, the H chemical shift of N—H were observed to be 11.33–13.56 ppm [42]. In the ^{13}C NMR spectra of the title compound, the signals observed at 146,49 ppm and 155,63 ppm due to C8 and C9 atoms of the triazole ring were calculated as 141.74 and 143.25 ppm, respectively. Table 5 shows the other calculated chemical shift values. As can be seen from Table 5, calculated ^{1}H and ^{13}C chemical shift values of the title compound are generally agreement with the experimental ^{1}H and ^{13}C shift data.

3.5. Molecular electrostatic potential

MEP at the B3LYP/6-31G(d) optimized geometry was calculated. MEP is shown in Fig. 8. Following the approach previously reported [43]. Here, the values of the MEP, which belong to the surface built by the points with an electronic density $\rho(r)$ = 0.001 a.u, were used. The negative (red and yellow) and the positive (blue) regions in the MEP were related to electrophilic reactivity and nucleophilic reactivity, respectively. As can be seen in Fig. 8, the negative regions of the title compound **(3)** were observed around the carbonyl O1 atom, N5 atom of imidazole ring and N3 atom. If compared, the negative $V(r)$ values are −0.073 a.u. for N5 atom, −0.059 a.u. for O1 atom and −0.044 a.u. for N3 atom. $V(r)$ value for N5 atom is found in the most negative region, where the others are in less

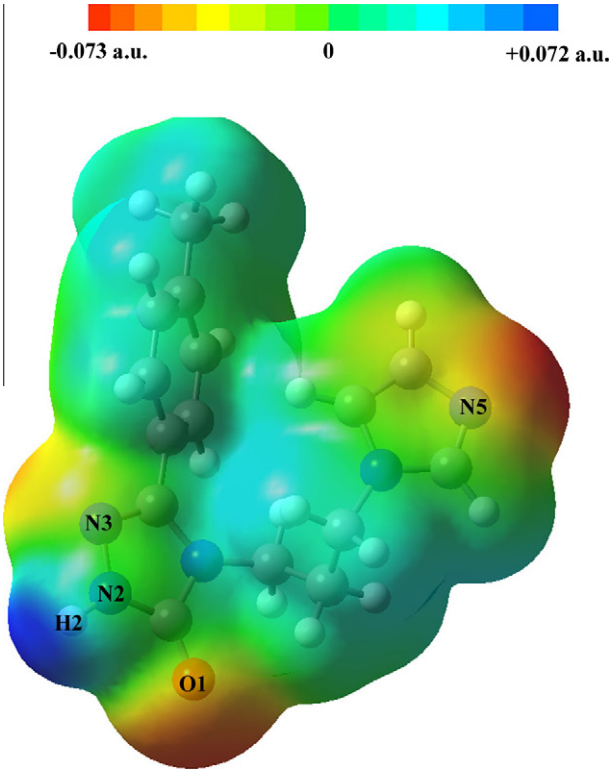

Fig. 8. Molecular electrostatic potential map calculated at B3LYP/6-31G(d) level.

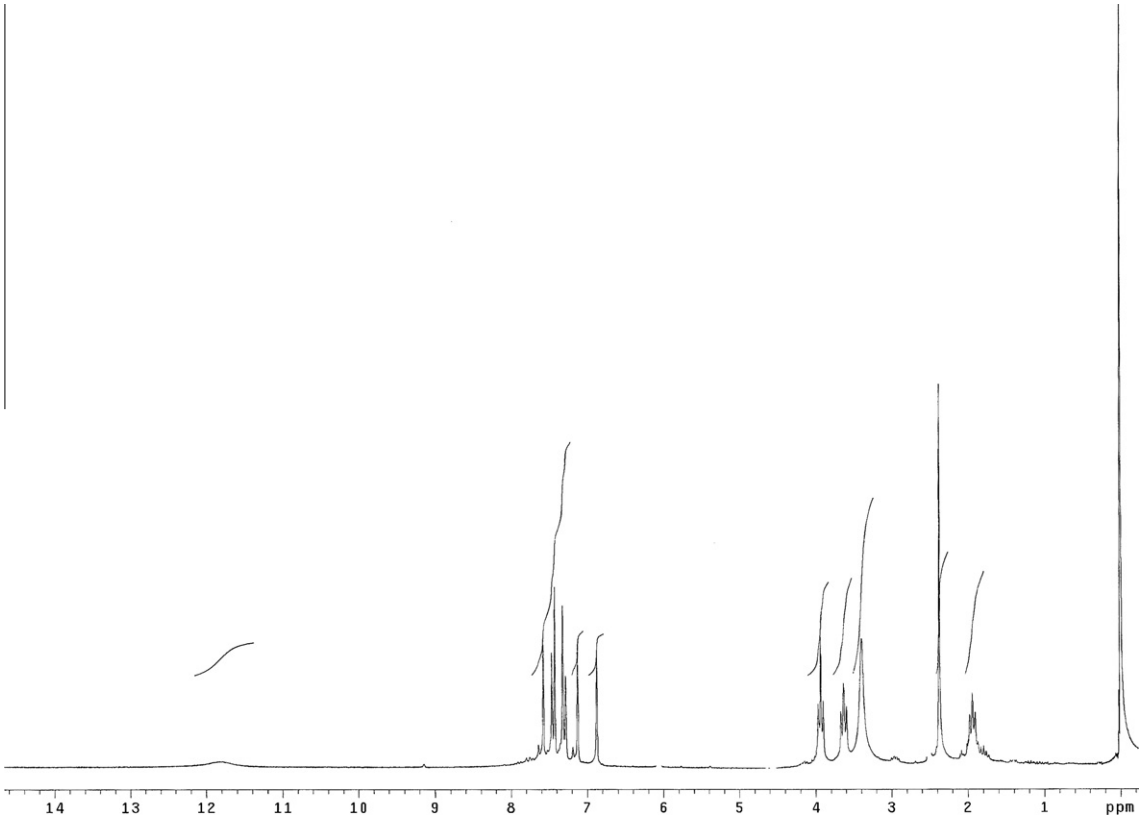

Fig. 7. The ^{1}H NMR spectra of the title compound (**3**).

negative region. A maximum positive region localized on the N2—H2 bond has value of +0.072 a.u. indicating a possible site for nucleophilic attack. Considering these calculated results, the MEP map shows that the negative potential sites are on electronegative, and positive potential sites around hydrogen atoms, respectively. These sites give the information about the region from where the compound can have intermolecular interactions. So, Fig. 8 confirms the existence of intermolecular N—H···N and C—H···O interactions.

3.6. Frontier molecular orbitals

The distributions and energy levels of the frontier molecular orbitals (FMOs) were computed at the B3LYP/6-31G(d) level for the title compound **(3)** and are shown in Fig. 9. As can be seen from Fig. 9, while LUMO + 1 is principally delocalized among the atoms of imidazol group, LUMO is delocalized among the atoms of both triazol and imidazol groups. HOMO − 1 orbitals mainly localized on the triazol and imidazol fragments, and HOMO is mainly localized on the benzene fragment. Both the highest occupied molecular orbitals (HOMOs) and the lowest-lying unoccupied molecular orbitals (LUMOs) are mainly localized on the rings indicating that the HOMO–LUMO are mostly the π-antibonding type orbitals [44]. The magnitude of the energy separation between the HOMO and LUMO is 4.97 eV. This large HOMO–LUMO gap is an indication of a good stability and a high chemical hardness for the title compound **(3)**, means high excitation energies for many of excited states.

4. Conclusions

4-(3-(1*H*-imidazol-1-yl) propyl)-5-*p*-tolyl-2*H*-1,2,4-triazol-3(4*H*)-one **(3)** has been synthesized and characterized by IR, NMR, and X-ray single-crystal diffraction. The crystal structure is stabilized by N—H···N and C—H···O type hydrogen bonds. X-ray, FT-IR and NMR spectral datas of the title compound **(3)** indicated that the compound exists as keto form. The theoretical calculations performed by DFT support the solid state structure. The conformational analysis study is considerably successful in determining the conformational preferring obtained from X-ray of the title compound **(3)**. The considerable differences between experimental and calculated results of IR and NMR can be attributed to the existence of N—H···N and C—H···O type intermolecular hydrogen bonds in the crystal structure. The MEP map shows that the negative potential sites are on oxygen atoms as well as the positive potential sites are around the hydrogen atoms and so MEP map confirms the existence of intermolecular N—H···N and C—H···O interactions. HOMO–LUMO gap with 4.97 eV indicates that the title compound **(3)** has a good stability and a high chemical hardness.

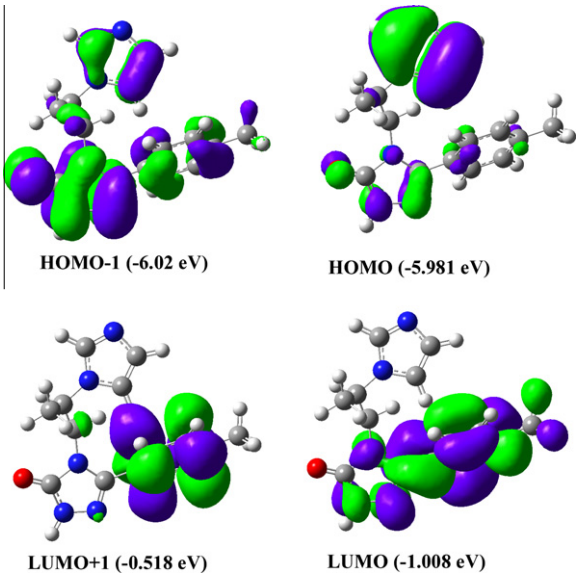

Fig. 9. Molecular orbital surfaces and energy levels given in parantheses for the HOMO − 1, HOMO, LUMO and LUMO + 1 of the title compound **(3)** computed at B3LYP/6-31G(d) level.

5. Supplementary data

CCDC-757066 contains the supplementary crystallographic data for the compound reported in this paper. These data can be obtained free of charge at www.ccdc.cam.ac.uk/conts/retrieving.html [or from the Cambridge Crystallographic Data Centre (CCDC), 12 Union Road, Cambridge CB2 1EZ, UK; fax: +44(0) 1223–336033; e-mail: deposit@ccdc.cam.ac.uk].

Acknowledgements

This study was supported by grants from Karadeniz Technical University (Project No: 2007.111.002.11) and the scientific and technological research council (TUBITAK Project No: 107T065) of Turkey.

References

[1] G. Heubach, B. Sachse Buerstell, H. Ger. Offen. 2 (1979) 760–826.
[2] G. Tanaka, Japan Kokai 973 (1974) 7495.
[3] D.A. Griffin, S.K. Mannion, Eur. Pat. Appl. EP 199 (1986) 474.
[4] N.B. Hanna, S.D. Dimitrijevich, S.B. Larson, R.K. Robsin, G.R. Revankar, J. Heterocycl. Chem. 25 (1988) 1857.
[5] B.T.C. Jenkins, I.J. Stratfort, Anticancer Drug Des. 4 (1989) 145–160.
[6] M.I. Husain, M. Amir, J. Indian Chem. Soc. 63 (1986) 317.
[7] S.H.L. Chiu, S.E.W. Huskey, Drug Metabol. Dispos. 26 (1998) 838.
[8] R. Eliott, R.L. Sunley, D.A. Griffin, UK Pat. Appl. GB 2 (1986) 175–301.
[9] P.E. Goss, K. Strasser-Weippl Best, Pract. Res. Clin. Endo. Met. 18 (2004) 113.
[10] Y. Ünver, E. Dugdu, K. Sancak, M. Er, Ş.A. Karaoglu, Turkish J. Chem. 33 (2009) 135.
[11] M. Clemons, R.E. Colemon, S. Verma, Cancer Treat. Rew. 30 (2004) 325.
[12] Y. Ünver, K. Sancak, H. Tanak, İ. Değirmencioğlu, E. Düğdü, M. Er, Ş. Işık, J. Mol. Struct. 936 (2009) 946.
[13] A. Narayana, D.R. Chapman, S.P. Upadhyaya, L. Bauer, J. Heterocycl. Chem. 30 (1993) 1404–1412.
[14] G. Menozzi, L. Mosti, C. Fossa, C. Murgioni, L.P. Colla, Farmaco 56 (2001) 633–640.
[15] K. Sancak, Y. Unver, H. Tanak, İ. Değirmencioğlu, E. Düğdü, M. Er, Ş. Işık, J. Incl. Phenom. Macrocycl. Chem. 67 (2010) 325–334.
[16] A.R. Katritzky (Ed.), Comprehensive Heterocyclic Chemistry II, A Review of the LITERATURE 1982–1995, vol.4, Elsevier Science Ltd., 1996, p. 127.
[17] Stoe Cie X-AREA (Version1.18) and X-RED32 (Version 1.04), Darmstadt, Germany, 2002.
[18] G.M. Sheldrick, SHELXS97 and SHELXL97 University of Göttingen, Germany, 1997.
[19] L.J. Farrugia, J. Appl. Cryst. 30 (1997) 565.
[20] L.J. Farrugia, J. Appl. Cryst. 32 (1999) 837–838.
[21] M.J. Frisch, G.W. Trucks, H.B. Schlegel, G.E. Scuseria, M.A. Robb, J.R. Cheeseman, J.A. Jr. Montgomery, J.T. Vreven, K.N. Kudin, J.C. Burant, J.M. Millam, S.S. Iyengar, J. Tomasi, V. Barone, B. Mennucci, M.Cossi, G. Scalmani, N. Rega, G.A. Petersson, H. Nakatsuji, M. Hada, M. Ehara, K. Toyota, R. Fukuda, J. Hasegawa, M. Ishida, T. Nakajima, Y. Honda, O. Kitao, H. Nakai, M. Klene, X. Li, J.E. Knox, H.P. Hratchian, J.B. Cross, V. Bakken, C. Adamo, J. Jaramillo, R. Gomperts, R.E. Stratmann, O. Yazyev, A.J. Austin, R. Cammi, C. Pomelli, J.W. Ochterski, P.Y. Ayala, K. Morokuma, G.A. Voth, P. Salvador, J.J. Dannenberg, V.G. Zakrzewski, S. Dapprich, A.D. Daniels, M.C. Strain, O. Farkas, D.K. Malick, A.D. Rabuck, K. Raghavachari, J.B. Foresman, J.V. Ortiz, Q. Cui, A.G. Baboul, S. Clifford, J. Cioslowski, B.B. Stefanov, G. Lui, A. Liashenko, P. Piskorz, I. Komaromi, R.L. Martin, D.J. Fox, T. Keith, M.A. Al-Laham, C.Y. Peng, A. Nanayakkara, M. Challacombe, P.M.W.B. Gill, B. Johnson, W. Chen, M.W. Wong,C. Gonzalez, J.A. Pople, GAUSSIAN 03, Revision C.02, Gaussian Inc., Wallingford, CT, 2004.
[22] P.J. Stephens, F.J. Devlin, C.F. Chablowski, M.J. Frisch, J. Phys. Chem. 98 (1994) 11623–11627.
[23] J.J.P. Stewart, J. Comput. Chem. 10 (1989) 209.
[24] J.J.P. Stewart, J. Comput. Chem. 10 (1989) 221.
[25] P. Politzer, S.J. Landry, T. Warnheim, Phys. Chem. 86 (1982) 4767, doi:10.1021/j100221a024.

[26] P. Politzer, L. Abrahmsen, P. Sjoberg, J. Am. Chem. Soc. 106 (1984) 855, doi:10.1021/ja00316a005.
[27] P. Politzer, P.R. Laurence, L. Abrahmsen, B.A. Zilles, P. Sjoberg, Chem. Phys. Lett. 111 (1984) 75, doi:10.1016/0009-2614(84)80439-X.
[28] J.S. Murray, P. Lane, T. Brinck, P. Politzer, P. Sjoberg, J. Phys. Chem. 95 (1991) 14.
[29] J.P. Merrick, D. Moran, L. Radom, J. Phys. Chem. A 111 (2007) 11683.
[30] A. Frisch, I.I.R. Dennington, T. Keith, J. Millam, A.B. Nielsen, A.J. Holder, J. Hiscocks GaussView Reference, Version 4.0, Gaussian Inc., Pittsburgh, 2007.
[31] R. Ditchfield, J. Chem. Phys. 56 (1972) 5688.
[32] K. Wolinski, J.F. Hinton, P. Pulay, J. Am. Chem. Soc. 112 (1990) 8251.
[33] P.J. Garratt, Comprehensive Heterocyclic Chemistry II, in: A.R. Katritzky, C.W. Rees, E.F.V. Scriven (Ed.), vol 4, Elsevier Science Ltd., 1996, pp. 127–163.
[34] F.H. Allen, O. Kennard, D.G. Watson, L. Brammer, A.G. Orpen, R.J. Taylor, J. Chem. Soc. Perkin Trans. 2 (1987) S1.
[35] R. Ustabaş, U. Çoruh, K. Sancak, E. Demirkan, E.M. Vázquez-López, Acta Cryst. E63 (2007) o2774–o2775.
[36] N. Ocak, B. Kahveci, S. Şaşmaz, E. Ağar, A. Erdönmez, Acta Cryst. E59 (2003) o1137–o1138.
[37] C. Peng, P.Y. Ayala, H.B. Schlegel, M.J. Frisch, J. Comput. Chem. 17 (1996) 49.
[38] A. Siwek, M. Wujec, I. Wawrzycka-Gorczyca, M. Dobosz, P. Paneth, Heteroatom Chem. 19 (2008) 337–344.
[39] Y. Ünver, K. Sancak, H. Tanak, I. Değirmencioğlu, E. Düğdü, J. Mol. Struct. 936 (2009) 46–55.
[40] H. Tanak, Y. Köysal, M. Yavuz, O. Büyükgüngör, K. Sancak, J. Mol. Model. 16 (2010) 447–457.
[41] D. Avcı, Y. Atalay, M. Şekerci, M. Dinçer, Spectrochim. Acta Part A 73 (2009) 212–217.
[42] P. Vainilavicius, R. Smicius, V. Jakubkiene, S. Tumkevicius, Manatshefte für Chemie 132 (2001) 825–831.
[43] P. Politzer, J. Murray, Theor. Chem. Acc. 108 (2002) 134.
[44] N. Özdemir, M. Dinçer, İ. Koca, O. Büyükgüngör, J. Mol. Model. 15 (2009) 1193–1201.